

K.V. Korytchenko, V.F. Bolyukh, S.G. Buriakovskiy, Y.V. Kashansky, O.I. Kocherga

Plasma acceleration in the atmosphere by pulsed inductive thruster

Introduction. One of the directions of development of plasma technologies consists in the formation of gas-metal plasma formations and throwing them to a certain distance. Known thrusters of plasma formation either have an electrode system that is prone to erosion, or a discharge system in a solid dielectric substance in which ablation occurs, or a complex gas-dynamic system with fuel supply. They do not provide acceleration of plasma formation in the atmosphere for a significant distance. **Purpose.** A theoretical and experimental study of electromechanical and thermophysical processes in a plasma thruster, which ensures the formation of a plasma formation due to thermal ionization by an induced current in a thin conductor layer during a high-voltage discharge on an inductor and the accelerating of a plasma formation in the atmosphere for a significant distance. **Methodology.** The proposed concept of a plasma thruster, in which the inductor inductively interacts with a combined armature, which includes an aluminum armature in the form of a thin (0.5-1 μm) foil, a copper armature made of a thicker foil (35-50 μm). On the basis of a mathematical model that takes into account the uneven distribution of currents in the inductor and conductive armatures, the features of the process of acceleration the combined armature in the atmosphere were established and experimental studies were carried out. **Results.** The electromechanical and thermal characteristics of the plasma thruster were calculated. It was established that the choice of the thickness of the dielectric layer of the armature, to which the aluminum and copper armatures are attached, is determined by the energy balance between the heating temperature of the aluminum armature and the electromechanical indicators of the thrower. **Scientific novelty.** It was experimentally established that the greatest density and homogeneity is observed in the middle of the plasma formation, which has the shape of a torus, moving away from the dielectric sheet on which the aluminum armature was located. As the voltage of the capacitive energy storage increases, the induced current density in the armature increases and the plasma formation becomes more uniform. **Practical value.** In comparison with the experimental results, the calculated current in the inductor coincides both in shape and in magnitude with an accuracy of 7%. The biggest difference between the calculated and experimental currents of the inductor occurs when the aluminum armature is thermally destroyed. The transition of an aluminum armature into a plasma formation depends significantly on the voltage of the capacitive energy storage. References 26, figures 16.

Key words: plasma formation pulsed inductive thruster, acceleration in the atmosphere, electromechanical and thermal processes, experimental research.

Вступ. Один з напрямків розвитку плазмових технологій полягає у формування газо-металевих плазмових утворень та метанні їх на певну відстань. Відомі металіки плазмового утворення або мають електродну систему, яка схильна до ерозії, або розрядну систему в твердій діелектричній речовині, в якій відбувається абляція, або складну газодинамічну систему з подачею палива. Вони не забезпечують метання плазмового утворення в повітряному середовищі на значну відстань. **Мета.** Теоретичне та експериментальне дослідження електромеханічних та теплофізичних процесів в металіку плазми, який забезпечує формування плазмового утворення за рахунок термічної іонізації індукованим струмом в тонкому провідниковому шару при високоевольтному розряді на індуктор та метання плазмового утворення у повітряному середовищі на значну відстань. **Методика.** Запропонована концепція металіку плазмового утворення, у якого індуктор індукційно взаємодіє з комбінованим якорем, що включає алюмінієвий якір у вигляді тонкої (0,5-1 мкм) фольги, мідний якір, який виконаний з більш товстої фольги (35-50 мкм). На базі математичної моделі, яка враховує нерівномірний розподіл струмів в індукторі і електропровідних якорях, встановлені особливості процесу метання комбінованого якоря в повітряному середовищі та проведені експериментальні дослідження. **Результати.** Розраховані електромеханічні і теплові характеристики плазмового металіку. Встановлено, що, вибір товщини діелектричного шару якоря, до якого прикріплені алюмінієвий і мідний якоря, обумовлений енергетичним балансом між температурою нагріву алюмінієвого якоря і електромеханічними показниками металіку. **Наукова новизна.** Експериментально встановлено, що найбільша густина і однорідність спостерігається в середині плазмового утворення, яке має форму тора, що віддаляється від діелектричного листа, на якому розташовувався алюмінієвий якір. З підвищенням напруги ємнісного накопичувача енергії збільшується густина індукваного струму в якорі і плазмове утворення стає більш однорідним. **Практична цінність.** У порівнянні з експериментальними результатами розрахований струм в індукторі співпадає як за формою, так і за значенням з точністю до 7%. Найбільша відмінність між розрахунковим і експериментальним струмами індуктора виникає при термічному руйнуванні алюмінієвого якоря. Перехід алюмінієвого якоря в плазмове утворення суттєво залежить від напруги ємнісного накопичувача енергії. Бібл. 26, рис. 16.

Ключові слова: плазмове утворення, імпульсний індуктивний металік, прискорення в атмосфері, електромеханічні та теплові процеси, експериментальні дослідження.

Introduction. Plasma technologies are used in various industrial technologies, in scientific research, in defense systems, etc. One of the directions of development of such technologies consists in the formation of plasma formations and accelerating them to a certain distance. Work on the creation of plasma throwers is being carried out in many scientific centers of the world [1-4].

At the University of Missouri, USA, the accelerating of a plasma formation in the air environment is being studied [5]. But the duration of the existence of a plasma formation is short (several ms), and it moves in the atmosphere for an insignificant distance of 0.5-0.6 m.

In [6], the application and development of plasma thrusters are considered. Electrode designs, discharge

patterns, fuel supply and ignition methods are analyzed. The authors consider various methods of modeling the discharge circuit, as well as the processes of ablation, ionization, and acceleration of plasma formation.

Pulsed plasma thrusters, in which high-frequency accelerating of plasma formation occurs, are considered for use in small satellites, because they provide a long operating time, high specific thrust impulse and significant power [7]. Such plasma thrusters are relatively easily adapted to the specific requirements of the satellite mission.

A promising direction in the development of thrusters for space vehicles is the development of plasma thrusters without electrodes, which are prone to plasma erosion [8, 9]. Such thrusters are more durable, have a reduced mass of

fuel compared to chemical ones, which create the same thrust. Electrodeless plasma thrusters include devices that provide a rotating magnetic or electric field, pulsed inductive devices that use the Lorentz force acting on induction currents in the plasma. According to the indicators of specific impulse and traction efficiency, the most promising designs are those that use the Lorentz force, which directly ensures the acceleration and throwing of plasma through magnetic nozzles.

Plasma technologies are actively developing and play an important role in many developing fields, such as medicine, agriculture, processing of materials and surfaces, catalysis, aerospace engineering, etc. [10].

Plasma thruster analysis. Let's consider the state of work on the creation of plasma thrusters that work in pulse mode and plasma thrusters that work for a long time in cyclic high-frequency mode.

In [11], the method of formation of plasma formations under the conditions of a high-voltage discharge in the atmosphere using a needle electrode is investigated. It was established that the presence of hemispherical aluminum foil can increase the electric field at the tip of the needle electrode. During a discharge under the action of a gas flow, an arc tip is formed in the electric field on the electrode. It forms a plasma jet that extends into the outer space of the gas nozzle. The pulsed discharge, which is formed by the interelectrode arc, forms a plasma jet of high density.

In [12], a plasma thruster with electrodes is considered, one of which is made in the form of a copper rod, and the other in the form of a plate. Under the action of an electric discharge between the electrodes in a solid dielectric substance, ablation occurs, that is, the substance evaporates from the surface. The plasma thruster works under low gas pressure in the accelerator channel. This thruster of plasma formation has a low efficiency and specific power, which is due to the use of only the energy stored by the electric field. The effectiveness of this thruster is limited by the long process of recovery of the working substance and the unevenness of its evaporation.

A well-known plasma thruster, which contains electrodes connected through an ohmic and inductive load to capacitive energy storage (CES), an end ceramic insulator that separates the electrodes and dielectric checkers installed between the electrodes, made of the material in which the ablation takes place [13]. When a high-voltage pulse is applied to the electrodes, as a result of a surface breakdown, a plasma formation is formed, which short-circuits the electrodes. The working substance that evaporates from the surface of the dielectric checkers is ionized and moved under the influence of electromagnetic forces and gas-dynamic pressure. This thruster has increased efficiency due to the use of both electromagnetic forces and gas-dynamic pressure. However, it has a low specific power due to the use of electrical energy to create electromagnetic and gas-dynamic forces.

A well-known plasma thruster, which consists of a guide tube covered by a magnet made in the form of sections, and a system of thermal ionization of matter to the plasma state [14]. One end of the pipe is in the atmosphere, and on the other end there is a gas flow formation system using a gas turbine engine. The system of thermal

ionization of matter consists of discharge electrodes located inside the guide tube and an induction plasma heater. The electromagnetic coil of the heater, which covers the guide tube, ensures the formation of plasma inside the guide tube. Due to the gas turbine engine, a heated gas flow is formed, which is directed into the guide pipe. Gas heated above 1000 °C is sent to the thermal ionization system, where it is heated by arc discharges to a high temperature (5000-10000 °C). The gas enters the region of the induction heater, where plasma formation occurs. Under the action of pulsed magnetic fields alternately created by sections of the magnet along the guide tube, a plasma formation is thrown.

In [15], the pulsed inductive thruster of plasma formation is considered, in which a high specific power is achieved due to the combined use of the chemical energy of fuel combustion and the energy of the electromagnetic field. This electrodeless thruster works by passing a large pulsed current through an inductor, creating an electromagnetic field that induces a current in the plasma and accelerates it to a high speed. The authors have proposed and tested different configurations of the thruster, which provide plasma throwing and use a magnetic field to hold it during acceleration. But this thruster has too complicated a design.

In [16], the pulsed inductive plasma thruster designed for a spacecraft is investigated. Spatial distributions of various physical fields are considered, which describe the evolution of the structure of the plasma current layer, the relationship between the traction force and the excitation current, the efficiency of the magnetic connection between the plasma and the excitation circuit, and the energy conversion process. The positive contribution of the secondary current layer to the maximum thrust of the thruster is shown. Oppression the initial gas to the inductor surface and improving its radial homogeneity can help strengthen the coupling between the plasma and the inductor. But the grounded metal plate on which the CES is attached can impair the process of plasma acceleration if the CES is in the zone of magnetic connection with the inductor.

Work [17] analyzes the circuits of the pulsed inductive plasma thruster with conical inductor coils, which can have cone angles from 0° (straight theta-pinch coil) to 90° (flat coil). The plasma is considered as a deformed projectile that moves radially and axially under the action of the electrodynamic force from the side of the inductor. A local maximum of the efficiency and specific impulse is found for angles less than 90°, but the absolute maximum for both of these values is observed at an angle of 90°.

In [18], a high-voltage pulsed power source for the formation of plasma in the atmosphere is considered. This photovoltaic-driven source provides voltage pulse widths from 1 μs to 10 μs and amplitudes in excess of 10 kV with frequencies from 0.5 kHz to 5 kHz.

In [19], the physical process of a planar induction-pulse plasma thruster was studied. When the environment was filled with argon as a fuel, the shape of the current in the inductor, the CES voltage, the intensity of the plasma radiation were measured, and photographs of the plasma structure were taken. Processes at different values of CES voltage and gas pressure were studied. Based on the results of the experiments, the physical mechanisms of the

initial phase of ionization and the subsequent phase of plasma formation acceleration were analyzed.

Based on the analysis, it can be concluded that known thrusters for the plasma formation of either have an electrode system that is prone to erosion, or a discharge system in a solid dielectric substance in which ablation occurs, or a complex gas-dynamic system with the supply of appropriate fuel. In addition, known thrusters, forming the plasma, do not ensure its accelerating in the atmosphere for a significant distance.

The purpose of the article is a theoretical and experimental study of electromechanical and thermophysical processes in a plasma thruster, which ensures the formation of a gas-metal plasma due to thermal ionization by an induced current in a thin conductor layer during a high-voltage discharge on an inductor and the accelerating of a plasma formation in the atmosphere for a considerable distance.

The concept of a pulsed inductive plasma thruster.

As it was shown in [20], when using CES with a relatively low voltage ($U_0 = 20$ kV, capacity $C_0 = 360$ μ F), an aluminum armature with a thickness of 18 μ m is only partially transformed into a plasma formation. A large part of this armature is moved vertically upwards to a considerable height (more than 5 m) and after testing the armature is a crumpled and compressed aluminum foil with a bunch of small particles. It is these elements of the armature, which have not passed into the plasma state, under the action of electrodynamic forces from the side of the inductor, are moved to a considerable distance. It was established that at the same CES voltage, only a part of the aluminum armature went into the plasma state, while the copper armature did not go at all. This can be explained by the fact that the melting point of aluminum (660 $^{\circ}$ C) is significantly lower than that of copper (1083 $^{\circ}$ C).

On the basis of these experimental studies, a pulsed inductive plasma thruster is proposed, in which a combined armature is located opposite the disc-shaped inductor, which includes an aluminum armature adjacent to the inductor and made in the form of a thin (0.5-1 μ m) foil, a copper armature that is directed in the direction of throwing and made of a thicker foil (35-50 μ m). These armatures are attached to the dielectric layer located between them (Fig. 1). This layer can be made of aerogel, which has a low density (1 kg/m^3), is resistant to high temperature (1000 $^{\circ}$ C), has a low thermal conductivity ($\lambda = 0.013\sim 0.019$ $\text{W}/(\text{m}\cdot\text{K})$), a low Young's modulus, does not compress and is resistant to deformation [21].

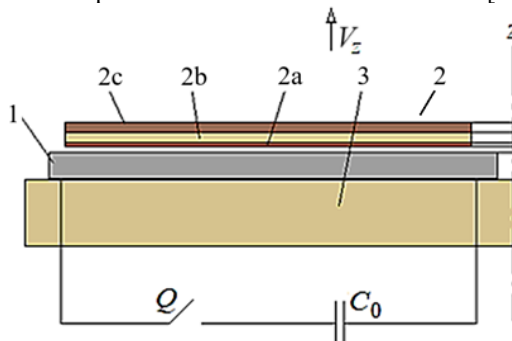


Fig. 1. Design scheme of a pulsed inductive plasma thruster: 1 – inductor; 2 – combined armature; 2a – aluminum armature; 2b – dielectric layer; 2c – copper armature; 3 – insulating support

When the inductor is excited by the high-voltage CES C_0 , induced currents flow in the conductive armatures. In a thinner aluminum armature, due to a higher density of the induced current and a lower melting temperature, thermal ionization and the transition to plasma formation occur. The thickness of the aluminum armature is significantly less than the depth of the skin layer. In a thicker copper armature, thermal ionization does not occur due to the reduced magnetic field of the inductor, lower induced current density and higher melting temperature. Under the action of electrodynamic forces, the plasma formation from the aluminum armature is pressed against the dielectric layer, and the copper armature connected to this layer is moved to a considerable distance from the inductor under the action of electrodynamic forces. The copper armature, taking on the aerodynamic resistance of the atmosphere, moves the dielectric layer attached to it with plasma formation, protecting the latter from intense cooling. The dielectric layer of the armature keeps the plasma formation in the form of a ring from being «ruptured» by radially directed electrodynamic forces.

Combined armatures formed from two electrically conductive armatures located in parallel, one of which can be stationary, are used in electromechanical pulse accelerators [22, 23]. These armatures do not go into a plasma formation due to high temperature, but move to a considerable distance.

A mathematical model that describes electromechanical and thermophysical processes during the accelerating of a plasma formation is presented in [20]. The thruster has a coaxial design and the combined armature moves along the z -axis at a speed of V_z . Since plasma formation is characterized by the uncertainty of dynamically changing parameters, in order to establish the general characteristics of the process, we consider that electrically conductive armatures do not change their shape and aggregate state during operation. This approach is widely used when calculating the electromechanical processes of a plasma thruster [24]. To implement a mathematical model that describes time-varying processes with spatially distributed parameters, a system of partial differential equations with respect to spatial and temporal variables was used [22]. The mathematical model describes the stress of the electrical support of the inductor and the combined armature as a function of temperature.

The mathematical model of the process of accelerating a combined armature in the atmosphere takes into account the uneven distribution of currents in the inductor and conductive armatures. It is implemented in the COMSOL Multiphysics software package using the finite element method when accounting for all relationships between physical processes. At the same time, data is exchanged between processes, calculation areas are allocated for each physical problem, provided that the grid division is consistent for all problems.

The calculation area of the model is a cylinder with a radius whose value is more than 5 times greater than the radius of the furthest element of the thrower in the radial direction from the z axis. The height of the calculated cylinder is more than 10 times greater than the highest height of the thruster elements. This makes it possible to

achieve the required accuracy with an acceptable calculation time, considering the calculation limit to be conditionally infinite.

Electromechanical and thermal processes in pulsed inductive plasma thruster with combined armature. Consider a plasma thruster with the following parameters: CES: voltage $U_0=35$ kV, capacity $C_0=18.5$ μ F; **inductor**: shape – Archimedes disk spiral, material – steel, number of turns $N_1=5$, outer diameter $D_{ex1}=280$ mm, inner diameter $D_{in1}=70$ mm, width of turn $\Delta r_1=10$ mm, high turn $h_1=5$ mm, distance between turns 10 mm; **combined armature**: outer diameter $D_{ex2}=280$ mm, inner diameter $D_{in2}=0$ mm, thickness of aluminum armature $h_{2a}=0.7$ μ m; distance from the inductor $z_0=1$ mm; **excitation circuit**: $L_0=1.5$ μ H, $R_0=105$ m Ω .

The current density in the turns of the steel inductor is distributed significantly unevenly. In Fig. 2 shows the distribution of the current density in the turns of the inductor j_1 at maximum current and the absence of an armature.

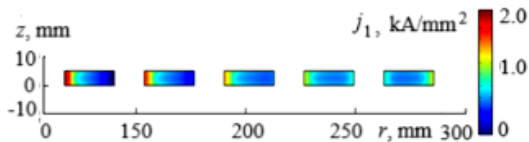


Fig. 2. Distribution of the current density in the turns of the inductor j_1 at the maximum current

The highest current density is observed on the inner coil, namely on the side facing the center, and the lowest current density is observed on the outer side of the inner coil. When calculating processes over time, we will use the current density averaged over the cross section of the turn.

Let us consider the mentioned processes in the plasma thruster with small ($h_{2b}=1$ mm) and large ($h_{2b}=15$ mm) thickness of the dielectric layer and with the thickness of the copper armature $h_{2c}=0.05$ mm. The currents in the inductor have an oscillating and decaying character over time (Fig. 3). With a small thickness of the h_{2b} dielectric layer, the amplitude of the first half-period is 17 % larger, and the oscillation period is reduced compared to the variant with a large h_{2b} thickness. This is due to the inductive effect of the copper armature, which strengthens the magnetic connection with the inductor.

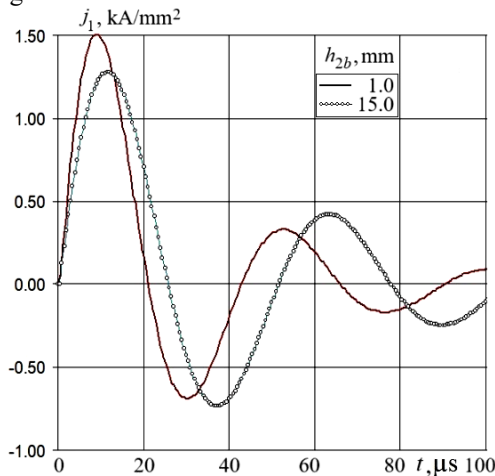


Fig. 3. Time dependences of the current density in the inductor

The amplitude of the density of the induced current in the copper armature j_{2c} increases by 53 % with a

smaller thickness ($h_{2b}=1$ mm) of the dielectric layer of the armature compared to the version with a greater thickness ($h_{2b}=15$ mm) (Fig. 4).

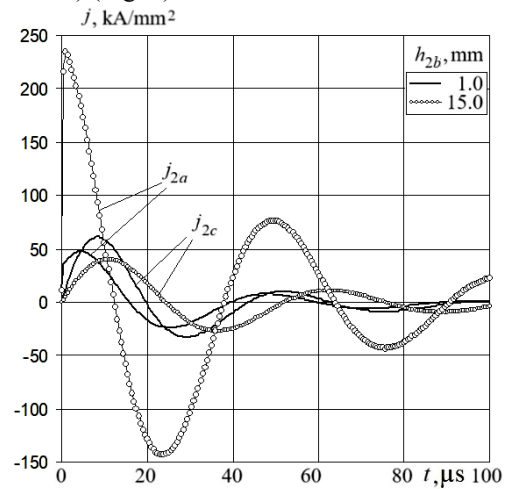


Fig. 4. Time dependences of current density in aluminum j_{2a} and copper j_{2c} armatures

But the amplitude of the current density in the aluminum armature j_{2a} decreases by almost 5 times, which does not lead to its thermal ionization. Such a change in the currents in the armatures is caused primarily by the influence of a thicker copper armature due to the induction connection with the inductor. When the copper armature moves away from the inductor, its demagnetizing effect on the aluminum armature weakens, which leads to a significant increase of induced current in the aluminum armature.

In Fig. 5 shows temperature extremes of aluminum $\theta_{2a}=T_0-T_{2a}$ and copper $\theta_{2c}=T_0-T_{2c}$ armatures, where T_0 is the temperature of the air medium, T_{2a} , T_{2c} are the temperature of the aluminum and copper armature, respectively.

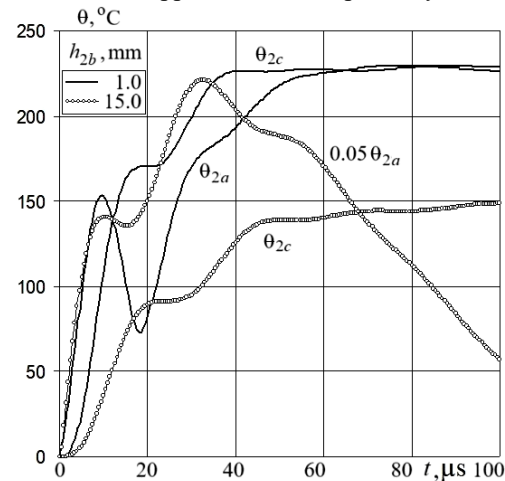


Fig. 5. Time dependences of temperature rise in aluminum θ_{2a} and copper θ_{2c} armatures

At a significant distance ($h_{2b}=15$ mm) of a thicker copper armature ($h_{2c}=50$ μ m) from a thinner aluminum armature ($h_{2a}=0.7$ μ m), the aluminum armature is heated to a temperature whose maximum excess $\theta_{2a}=4420$ $^{\circ}$ C is many times higher than the temperature aluminum smelting. With a small distance between the armatures ($h_{2b}=1$ mm), the maximum heating of the aluminum armature reaches only $\theta_{2a}=229$ $^{\circ}$ C and does not lead to its

thermal damage. Note that both at large and at small distances between the h_{2b} armatures, the heating of the copper armature does not exceed its melting point.

But when the copper armature is moved away from the aluminum one, the electromechanical indicators of the thruster significantly deteriorate. As calculations show, the resulting electrodynamic force f_z acting on the combined armature consists of more than 97 % of the force acting on the thicker copper armature. When the thickness of the dielectric layer h_{2b} increases from 1 mm to 15 mm, the maximum magnitude of the electrodynamic force decreases by 2.48 times, which leads to a decrease in the maximum speed of the armature V_z by 1.75 times (Fig. 6).

Thus, the choice of the thickness of the dielectric layer h_{2b} of the armature is due to a compromise between the high heating temperature of the aluminum armature and low electromechanical indicators of the thruster at a significant value of $h_{2b}=15$ mm and high electromechanical indicators and low heating temperature of the aluminum armature at a small value of $h_{2b}=1$ mm.

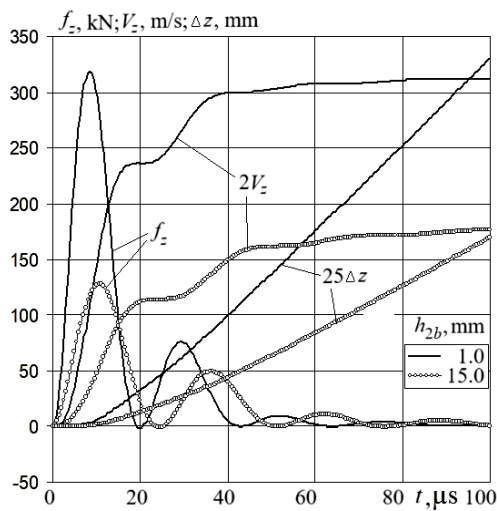


Fig. 6. Time dependences of electromechanical parameters of the thruster

Let's consider the effect of the thickness of the dielectric layer h_{2b} on the indicators of a thruster whose copper armature has a small (0.01 mm), medium (0.05 mm) and significant (0.5 mm) thickness h_{2c} . In Fig. 7 shows the dependence of the maximum current density j_m , the maximum electrodynamic force f_{zm} and speed V_{zm} , the maximum temperature rise θ_m of the armatures on the thickness of the dielectric layer h_{2b} between them.

When the thickness of the dielectric layer h_{2b} of the armature increases, the maximum current density in the aluminum armature j_{2a} increases, and in the copper armature j_{2c} it decreases (Fig. 7,a).

If in a copper armature, the smaller its thickness, the greater the maximum current density, then in an aluminum armature there is no such unequivocal relationship. Since the main electromechanical characteristics of the thruster are determined by the copper armature, when the thickness of the dielectric layer h_{2b} increases, that is, when the copper armature is moved away from the inductor, the maximum value of the electrodynamic force f_{zm} and the maximum speed V_{zm} decrease (Fig. 7,b). When the thickness of the h_{2c} copper armature increases, the total weight of the armature

increases significantly, almost proportionally. At the same time, the maximum force f_{zm} increases, and the maximum speed V_{zm} decreases.

When the thickness of the dielectric layer h_{2b} increases, the maximum temperature rise θ_{2c} of the copper armature decreases due to a decrease in the induced current (Fig. 7,c).

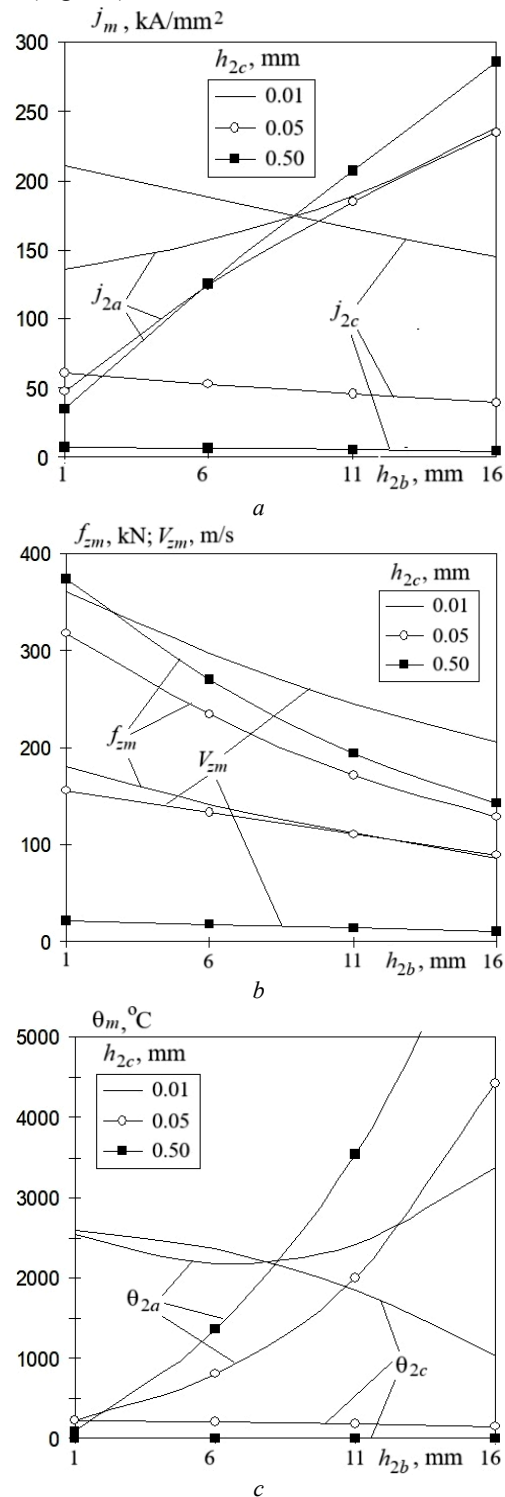


Fig. 7. Dependence of the maximum current density (a), the maximum electrodynamic force and speed (b), and the maximum temperature rise of the armatures (c) on the thickness of the dielectric layer h_{2b}

And an increase in the thickness of the copper armature h_{2c} reduces the density of the induced current, and

accordingly, the maximum value of the temperature rise θ_{2c} . But with the maximum excess temperature of the aluminum armature θ_{2a} , there is no such unequivocal dependence.

When the copper armature with a thickness of $h_{2c}=0.05$ mm or 0.5 mm is moved away, the temperature rise of the aluminum armature increases, and more at $h_{2c}=0.5$ mm. And when the copper armature has a small thickness $h_{2c}=0.01$ mm, when the thickness of the dielectric layer h_{2b} increases from 1 mm to 6 mm, the maximum excess temperature of the aluminum armature θ_{2a} decreases with a further relatively insignificant increase.

The conducted studies took into account the invariance of the mechanical state of the aluminum armature. But, as shown by calculations using a mathematical model that takes into account the thermal destruction of an aluminum armature at a temperature above 660 °C, the results practically do not differ from the results described above. This is explained by the fact that the thicker (71.5 times) copper armature than the aluminum one mainly determines the electromechanical processes of the thrower. The confirmation of this statement is the results of the calculations of the thruster, which includes only one aluminum armature, which causes a certain distortion of the current shape of the inductor until the moment of thermal damage of the armature.

Experimental studies. To test the proposed concept of plasma acceleration by pulsed inductive thruster in the atmosphere on the basis of the high-voltage electrophysical stand of the Research and Design Institute «Molniya» of National Technical University «Kharkiv Polytechnic Institute» using the methodology [25], experimental studies of a plasma formation thruster with one or a copper or aluminum armature in the form of a flat foil were conducted (Fig. 8).

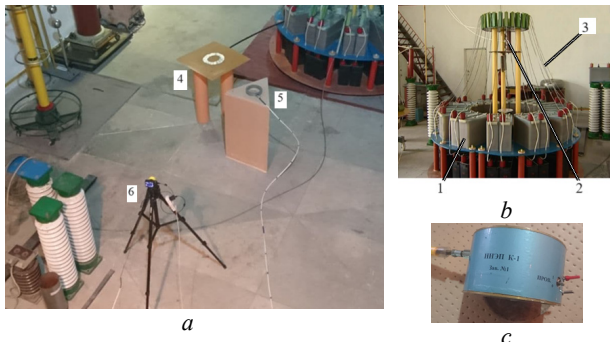


Fig. 8. Photo of the experimental setup (a), pulse source (b), electric field sensor (c): 1 – battery of pulse capacitors; 2 – high-voltage arrester; 3 – system of prefabricated tires; 4 – thruster of plasma formation; 5 – electric field sensor; 6 – high-speed camera

Experimental studies were carried out with two disc inductors, which are made in the form of an Archimedes disk spiral made of steel (Fig. 9). They have an outer diameter $D_{ex1}=280$ mm, an inner diameter $D_{in1}=70$ mm and a height $h_1=5$ mm. Inductor No. 1 has 7 turns with a width of 9.4 mm with a distance between turns of 5 mm. Inductor no. 2 has 5 turns with a width of 10 mm with a distance between turns of 10 mm. The inductor was placed horizontally on the dielectric base, and the conductive anchor through the dielectric sheet was installed on top of it.

The INEP K-1 sensor was used to measure the electric field strength, which is connected to a digital oscilloscope through a fiber optic cable (Fig. 8,c). It is located at a distance of 1 m from the center of the inductor. The measurement was carried out in the position of the maximum sensitivity of the sensor. A high-speed camera was located at a distance of 2.8 m from the center of the inductor to record the process of throwing the plasma formation (Fig. 8,a).

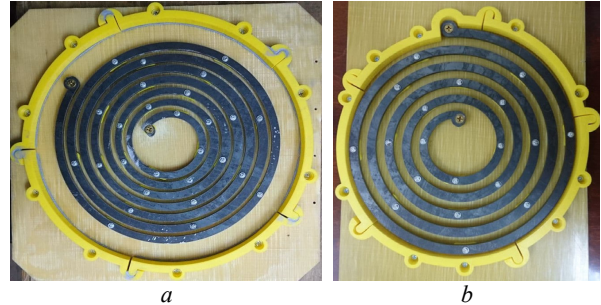


Fig. 9. Photo of inductor no. 1 (a) and inductor no. 2 (b)

In order to experimentally confirm the calculated results about the circular shape of the induced current in the conductive armature, the following experiment was conducted. A $900 \times 900 \times 1$ mm³ glass-textolite sheet, on the outside of which a copper foil with a thickness of 35 μ m was fixed, was placed above the horizontally located inductor no. 1. When a CES discharge with a voltage of $U_0=20$ kV was applied to the inductor in the fiberglass foil, which functions as a copper armature, a circular circuit of thermal heating was formed without significant mechanical damage. At the same time, the radial temperature distribution was in good agreement with the calculated results (Fig. 10). It should be noted that under similar conditions, thermal ionization took place in the aluminum armature with a transition to the plasma state and significant mechanical damage [20]. Based on this experiment, an aluminum armature was made in the form of a ring from foil 18 μ m thick (Fig. 10,c).

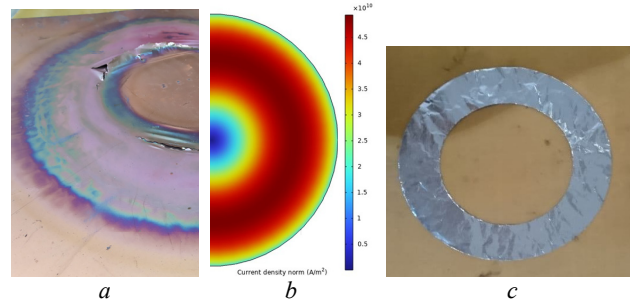


Fig. 10. Photo of the glass-textolite copper foil after the discharge of the inductor (a), calculated induced current (b) and photo of the aluminum armature (c)

In Fig. 11, with the CES voltage $U_0=40$ kV and the presence of an aluminum armature, the forms of the current in the inductor no. 2 and the electric field strength measured by the INEP K-1 sensor at the oscillograph sweep of 25 ms/div are shown on a digital oscilloscope.

The forms of the inductor current and the electric field have an oscillatory-damping character with a frequency of $f = 12.15$ kHz. The amplitude of the first half-cycle of the current is $I_{1m}=49.2$ kA, and the amplitude of the electric field intensity $E_m=430$ V/m.

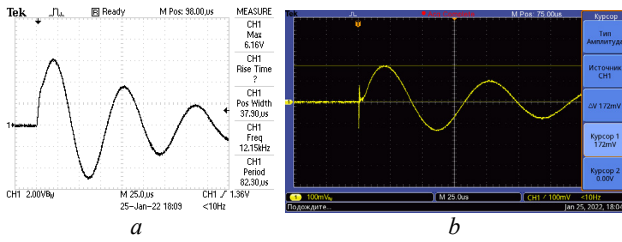


Fig. 11. Registered forms of current in inductor no. 2 (a) and electric field strength (b) in the presence of an aluminum armature and voltage $U_0=40$ kV

In the course of $5 \mu\text{s}$, in the form of the current of the inductor in the presence of an aluminum armature, there is a distortion from the similar form of the current in the absence of the armature. This is more pronounced when the sweep of the oscilloscope is reduced by 5 times (Fig. 12).

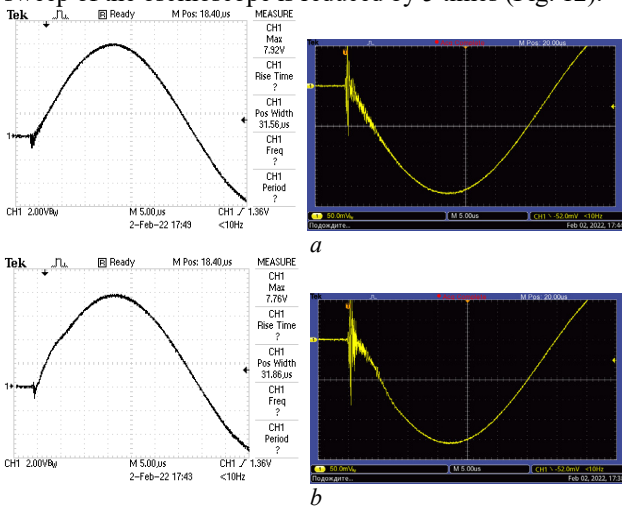


Fig. 12. Oscillograms of inductor current (left) and electric field strength (right) in the absence (a) and presence (b) of an aluminum armature

This distortion is explained by the inductive effect of the conductive armature and shows that for $5 \mu\text{s}$ there is an inductive interaction between the inductor and the armature. After this time, the induced current of the armature ceases to interact with the inductor both due to its movement and due to the fact that the aluminum armature is destroyed due to thermal ionization. The lack of interaction of the induced current in the armature with the inductor leads to the return of the inductor current curve to the state observed in the absence of the armature.

There is no specified distortion on the electric field intensity curve. This is explained by the fact that the sensor measures the combined electric field from the inductor and the armature, and the induced current in the armature is directed opposite to the inductor current, compensating for this distortion.

In Fig. 13 shows the calculated shape of the current density of the inductor j_1 and the aluminum armature j_{2a} , which is destroyed at a temperature higher than 660°C . It is the induction current in the armature that causes distortion in the inductor current curve. In comparison with the experimental dependence, the calculated current in the inductor coincides both in shape and in magnitude with an accuracy of 7 %.

The greatest difference between the expansion and experimental struts of the inductor arises in the process of thermal destruction of the aluminum armature.

At the stage of transition of the aluminum armature into the plasma mill, its support rapidly grows, which leads to a change in the shape of the pulse from oscillating and decaying character (Fig. 4) to “cut” with a short trailing edge (Fig. 13). When calculating the process of the transition to the plasma state, the resistance of the aluminum armature is described by a polynomial, which increases from a certain value up to the melting temperature ($\sim 550^\circ\text{C}$) to infinity when this temperature is exceeded ($\sim 700^\circ\text{C}$).

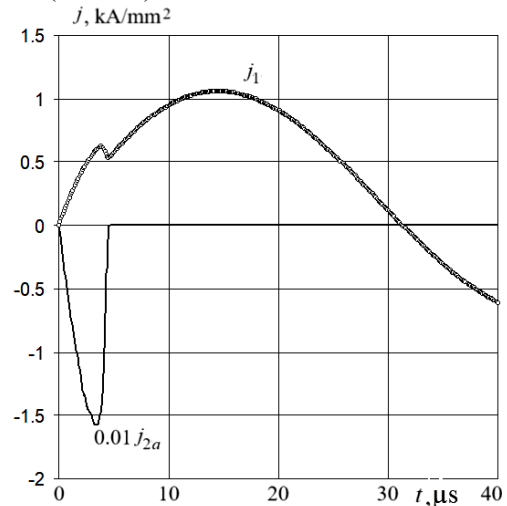


Fig. 13. Calculated form of current density of inductor j_1 and aluminum armature j_{2a}

As experimental studies show, the process of destruction of an aluminum armature occurs more slowly than it is laid down in the mathematical model.

The transition of the aluminum armature into a plasma formation depends significantly on the CES voltage U_0 . This is illustrated by Fig. 14, where photos taken without a light filter are shown of the plasma formation into which the aluminum armature has turned, at a voltage of $U_0=20$ kV, 30 kV and 40 kV.

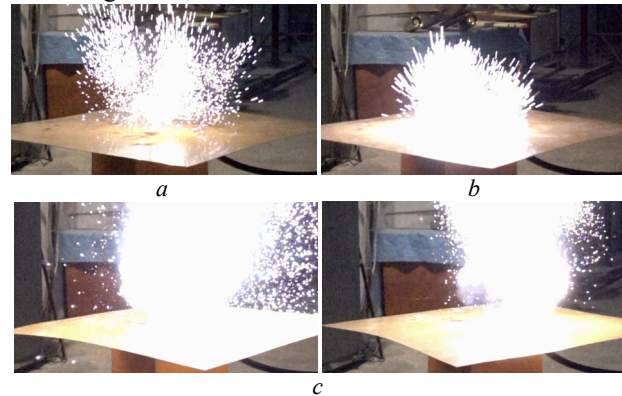


Fig. 14. Photos of plasma formation obtained at voltage U_0 : 20 kV (a), 30 kV (b), 40 kV (c), taken without a light filter

The measured inductor current amplitudes of the first half-cycle I_{1m} are 30.6 kA, 47 kA and 64.5 kA, respectively. The higher the density of the induced current in the armature, the more homogeneous the plasma formation. In this case, the duration of the induced current flow in the plasma formation increases. And due to the electrodynamic interaction of this current with the magnetic field of the inductor, the plasma formation is accelerating over a greater distance.

When using inductor no. 1, the amplitude of the first half-cycle of the inductor current, and therefore the density of this current, decreases. Thus, at a voltage of $U_0=40$ kV, the current amplitude is $I_{1m}=53$ kA (Fig. 15). At the same time, the greater part of the aluminum armature, in comparison with the similar voltage in the inductor no. 2, flies into the air environment in the form of a pile of small high-temperature particles.

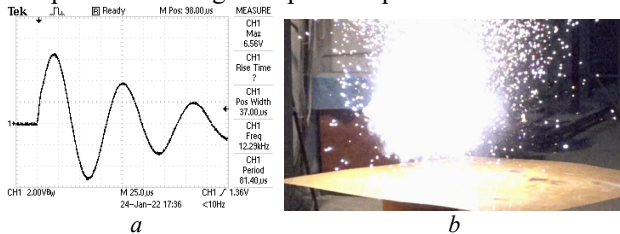


Fig. 15. Recorded form of current in inductor no. 1 (a) and photo plasma formation (b) at voltage $U_0=40$ kV

In order to investigate the processes in the plasma formation in more detail, experiments were conducted with photographing them accelerating a light filter from welding glasses with 12 DIN dimming. In Fig. 16 shows a photo of a plasma formation with the use of a light filter and an oscillogram of the inductor current and electric field strength during an CES discharge with a voltage of $U_0=40$ kV on inductor no. 1.

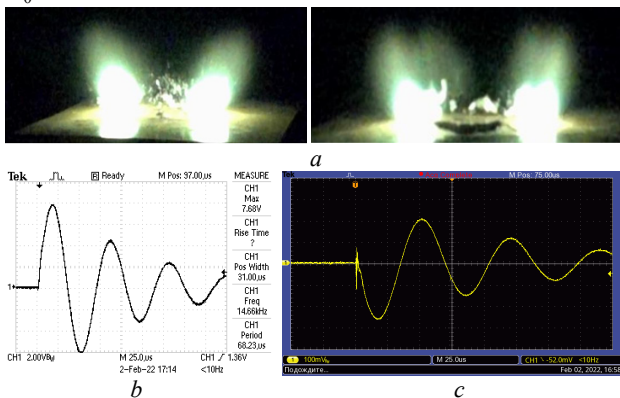


Fig. 16. Photo of plasma formation using a light filter (a), inductor current oscillogram (b) and electric field strength (c)

The amplitude of the first half-cycle of the inductor current is $I_{1m}=51.6$ kA, and the corresponding amplitude of the electric field strength is $E_m=450$ V/m. A photo using a light filter shows that the greatest density and uniformity is observed in the middle of the plasma formation. Moreover, it has the shape of a torus, which is separated from the dielectric sheet on which the aluminum armature was located.

Thus, the formation of gas-metal plasma formations and accelerating them to a certain distance contributes to the development of plasma technologies for promising areas of industry and scientific research. Among the directions of practical applications of throwing plasma formations formed during an induction discharge, one can note the possibility of their use in coating technologies, which are an alternative to vacuum electron beam methods for obtaining aluminum-copper compounds, as described, for example, in [26].

Conclusions.

1. The proposed concept of the plasma acceleration by pulsed inductive thruster in the atmosphere, in which a

combined armature is located opposite the inductor, which includes an aluminum armature made in the form of a thin foil, adjacent to the inductor, and a copper armature made of thicker foil, which is directed in the direction of accelerating. These armatures are attached to the dielectric layer of aerogel placed between them.

2. When using a mathematical model in the COMSOL Multiphysics software package, which takes into account interrelated electromechanical and thermal processes and uneven distribution of currents in the inductor and conductive armatures, it was established that under the action of electrodynamic forces from the inductor side, the copper armature moves a considerable distance, moving the attached to it is a dielectric layer with a plasma formation, into which the aluminum armature has turned.

3. It was established that the choice of the thickness of the dielectric layer of the armature is due to a compromise between the heating temperature of the aluminum armature and the electromechanical indicators of the thruster.

4. It was experimentally established that the greatest density and homogeneity is observed in the middle of the plasma formation, which has the shape of a torus, moving away from the dielectric sheet on which the aluminum armature was located.

5. As the voltage of the capacitive energy storage increases, the induced current density in the armature increases and the plasma formation becomes more uniform.

Conflict of interest. The authors declare that they have no conflicts of interest.

REFERENCES

1. Kirchen M., J alas S., Messner P., Winkler P., Eichner T., Hübner L., Hülsenbusch T., Jeppe L., Parikh T., Schnepf M., Maier A.R. Optimal Beam Loading in a Laser-Plasma Accelerator. *Physical Review Letters*, 2021, vol. 126, no. 17, art. no. 174801. doi: <https://doi.org/10.1103/PhysRevLett.126.174801>.
2. Albert F., Couprie M.E., Debus A., et al. 2020 roadmap on plasma accelerators. *New Journal of Physics*, 2021, vol. 23, no. 3, art. no. 031101. doi: <https://doi.org/10.1088/1367-2630/abcc62>.
3. Ji H., Daughton W. Phase diagram for magnetic reconnection in heliophysical, astrophysical, and laboratory plasmas. *Physics of Plasmas*, 2011, vol. 18, no. 11, pp. 111207-111217. doi: <https://doi.org/10.1063/1.3647505>.
4. Korytchenko K.V., Bolyukh V.F., Rezinkin O.L., Burjakovskij S.G., Mesenko O.P. Axial coil accelerator of plasma ring in the atmospheric pressure air. *Problems of Atomic Science and Technology*, 2019, vol. 119, no. 1, pp. 120-123.
5. Anthony S. Open-air plasma device could revolutionize energy generation, US Navy's weaponry. Available at: <https://www.extremetech.com/defense/153630-open-air-plasma-device-could-revolutionize-energy-generation-us-navys-weaponry> (accessed 08.01.2024).
6. Wu Z., Huang T., Liu X., Ling W.Y.L., Wang N., Ji L. Application and development of the pulsed plasma thruster. *Plasma Science and Technology*, 2020, vol. 22, no. 9, art. no. 094014. doi: <https://doi.org/10.1088/2058-6272/aba7ac>.
7. Ling W.Y.L., Zhang S., Fu H., Huang M., Quansah J., Liu X., Wang N. A brief review of alternative propellants and requirements for pulsed plasma thrusters in micropropulsion applications. *Chinese Journal of Aeronautics*, 2020, vol. 33, no. 12, pp. 2999-3010. doi: <https://doi.org/10.1016/j.cja.2020.03.024>.
8. Bathgate S.N., Bilek M.M.M., Mckenzie D.R. Electrodeless plasma thrusters for spacecraft: a review. *Plasma Science and Technology*, 2017, vol. 19, no. 8, art. no. 083001. doi: <https://doi.org/10.1088/2058-6272/aa71fe>.

9. Zhang Z., Ling W.Y.L., Tang H., Cao J., Liu X., Wang N. A review of the characterization and optimization of ablative pulsed plasma thrusters. *Reviews of Modern Plasma Physics*, 2019, vol. 3, no. 1, art. no. 5. doi: <https://doi.org/10.1007/s41614-019-0027-z>.
10. Keidar M., Weltmann K.-D., Macheret S. Fundamentals and Applications of Atmospheric Pressure Plasmas. *Journal of Applied Physics*, 2021, vol. 130, no. 8, art. no. 080401. doi: <https://doi.org/10.1063/5.0065750>.
11. Li Z., Liu W. Erratum to: The Formation of Atmospheric Pressure Air Low Temperature Plasma Jet. *Plasma Physics Reports*, 2022, vol. 48, no. 12, pp. 1422-1422. doi: <https://doi.org/10.1134/S1063780X22330017>.
12. Spanjers G.G., McFall K.A., Gulczynski F.S., Spores R.A. Investigation of propellant inefficiencies in a pulsed plasma thruster. *32nd Joint Propulsion Conference and Exhibit*, 1996, doi: <https://doi.org/10.2514/6.1996-2723>.
13. Takahashi K. Magnetic nozzle radiofrequency plasma thruster approaching twenty percent thruster efficiency. *Scientific Reports*, 2021, vol. 11, no. 1, art. no. 2768. doi: <https://doi.org/10.1038/s41598-021-82471-2>.
14. Di Canto G. *Plasma propulsion system and method*. Patent US WO2016151609. 2016. Available at: <https://patentscope.wipo.int/search/en/detail.jsf?docId=WO2016151609&cid=P10-LL70BV-97870-1> (accessed 08.01.2024).
15. Polzin K., Martin A., Little J., Promislow C., Jorns B., Woods J. State-of-the-Art and Advancement Paths for Inductive Pulsed Plasma Thrusters. *Aerospace*, 2020, vol. 7, no. 8, art. no. 105. doi: <https://doi.org/10.3390/aerospace7080105>.
16. Che B., Cheng M., Li X., Guo D. Physical mechanisms and factors influencing inductive pulsed plasma thruster performance: a numerical study using an extended magnetohydrodynamic model. *Journal of Physics D: Applied Physics*, 2018, vol. 51, no. 36, art. no. 365202. doi: <https://doi.org/10.1088/1361-6463/aad47f>.
17. Martin A.K. Performance scaling of inductive pulsed plasma thrusters with coil angle and pulse rate. *Journal of Physics D: Applied Physics*, 2016, vol. 49, no. 2, art. no. 025201. doi: <https://doi.org/10.1088/0022-3727/49/2/025201>.
18. Li M., Luo K., Xiong Z. Design of Adjustable High Voltage Pulse Power Supply Driven by Photovoltaic Cells for Cold Plasma Generation. *2021 IEEE 4th International Electrical and Energy Conference (CIEEC)*, 2021, pp. 1-6. doi: <https://doi.org/10.1109/CIEEC50170.2021.9510416>.
19. Li X.-K., Che B.-X., Cheng M.-S., Guo D.-W., Wang M.-G., Yang Y.-T. Investigation on plasma structure evolution and discharge characteristics of a single-stage planar-pulsed inductive accelerator under ambient fill condition. *Chinese Physics B*, 2020, vol. 29, no. 11, art. no. 115201. doi: <https://doi.org/10.1088/1674-1056/ab9f2a>.
20. Korytchenko K.V., Bolyukh V.F., Buriakovskiy S.G., Kashansky Y.V., Kocherga O.I. Electromechanical and thermophysical processes in the pulse induction accelerator of plasma formation. *Electrical Engineering & Electromechanics*, 2023, no. 5, pp. 69-76. doi: <https://doi.org/10.20998/2074-272X.2023.5.10>.
21. *Aerogel*. Available at: <https://en.wikipedia.org/wiki/Aerogel> (accessed 08.01.2024).
22. Bolyukh V.F., Kocherga A.I. Efficiency and Practical Implementation of the Double Armature Linear Pulse Electromechanical Accelerator. *2021 IEEE 2nd KhPI Week on Advanced Technology (KhPIWeek)*, 2021, pp. 153-158. doi: <https://doi.org/10.1109/KhPIWeek53812.2021.9570065>.
23. Bolyukh V.F. Effect of electric conducting element on indicators of linear pulse electromechanical converter induction type. *Technical Electrodynamics*, 2020, no. 3, pp. 22-29. doi: <https://doi.org/10.15407/techned2020.03.022>.
24. Polzin K.A., Sankaran K., Ritchie A.G., Reneau J.P. Inductive pulsed plasma thruster model with time-evolution of energy and state properties. *Journal of Physics D: Applied Physics*, 2013, vol. 46, no. 47, art. no. 475201. doi: <https://doi.org/10.1088/0022-3727/46/47/475201>.
25. Janda M., Korytchenko K., Shypul O., Krivosheev S., Yeresko O., Kasimov A. Optical and electrical investigation of plasma generated by high-energy self-stabilized spark ignition system. *Physics of Plasmas*, 2023, vol. 30, no. 5, art. no. 053501. doi: <https://doi.org/10.1063/5.0141261>.
26. Donets S.E., Klepikov V.F., Lytvynenko V.V., et al. Aluminum surface coating of copper using high-current electron beam. *Problems of Atomic Science and Technology*, 2015, vol. 98, no. 4, pp. 302-305.

Received 09.01.2024
Accepted 26.02.2024
Published 20.06.2024

K.V. Korytchenko¹, Doctor of Technical Science, Professor,
V.F. Bolyukh¹, Doctor of Technical Science, Professor,
S.G. Buriakovskiy², Doctor of Technical Science, Professor,
Y.V. Kashansky¹, Postgraduate Student,
O.I. Kocherga¹, PhD, Assistant Professor,
¹ National Technical University «Kharkiv Polytechnic Institute»,
2, Kyrpychova Str., Kharkiv, 61002, Ukraine,
e-mail: vfbolyukh@gmail.com (Corresponding Author);
² Research and Design Institute «Molniya»
of National Technical University «Kharkiv Polytechnic Institute»,
47, Shevchenko Str., Kharkiv, 61013, Ukraine.

How to cite this article:

Korytchenko K.V., Bolyukh V.F., Buriakovskiy S.G., Kashansky Y.V., Kocherga O.I. Plasma acceleration in the atmosphere by pulsed inductive thruster. *Electrical Engineering & Electromechanics*, 2024, no. 4, pp. 61-69. doi: <https://doi.org/10.20998/2074-272X.2024.4.08>